

# Energy optimization of high-rise commercial buildings integrated with photovoltaic facades in urban context

Xi Chen <sup>a\*</sup>, Hongxing Yang <sup>a</sup> and Jinqing Peng <sup>b</sup>

<sup>a</sup> Renewable Energy Research Group (RERG), Department of Building Services Engineering,  
The Hong Kong Polytechnic University, Kowloon, Hong Kong, China

<sup>b</sup> College of Civil Engineering, Hunan University, Changsha 410082, Hunan, China

## Abstract

This research thoroughly explored the impact of archetypes and confounding factors on a proposed holistic design optimization approach for high-rise office buildings with integrated photovoltaic (PV) facades. The design optimization adopts the hybrid generalized pattern search particle swarm optimization (HGPPSO) algorithm, which is incorporated with qualitative and quantitative sensitivity analyses for factor prioritizing and fixing. Different archetypes are modelled by changing floor plan sizes and shapes, while diverse urban contexts and internal load (heat gain) levels are investigated as major confounding factors beyond designers' control. Variation of these four simulation scenarios are then used to examine the uncertainty of sensitivity indices and optimization potential for passive architectural design parameters. The window geometry, thermal and optical properties are proved to be most important to the reference PV envelope design. The building plan shape is found to have little impact on the weighting of different design parameters, while the shape coefficient (SC) is determined to be almost linearly correlated with the HVAC (heating, ventilation and air-conditioning) demand. The office design with the highest shape coefficient can therefore achieve a net energy demand reduction up to 48.77%. The floor plan size also has minor impact on the sensitivity index for each design factor, but the energy-saving potential grows with decreasing floor sizes. On the contrary, confounding factors can greatly change the sensitivity analysis (SA) result. The window U-value becomes more important with an increasing internal load level and urban context density whereas the impact of the window light-to-solar gain ratio is reduced by peripheral shading. Furthermore, varying confounding factors can even change the dimension of optimization problems based on different factor fixing results. This research can

\* Corresponding author: Tel.: +852-2766 4726, Fax: 2765 7198, E-mail: [climber027@gmail.com](mailto:climber027@gmail.com)

provide early-stage design guidance for energy efficient buildings with a comprehensive analysis of pragmatic building archetypes, background contexts and operation scenarios.

*Keywords: Photovoltaic facade; Energy demand; Optimization; Passive architectural design; Archetype; Confounding factor*

## **1. Introduction**

Commercial buildings in Hong Kong are major energy consumers which account for more than 40% domestic energy consumption based on the statistics of Electrical & Mechanical Services Department (EMSD) [1]. Office buildings alone occupy more than 10% of the energy end-use in the whole commercial sector. To realize the sustainable development goal, Hong Kong Green Building Council launched the HK2030 Campaign to reduce at least 30% of the building energy use by 2030. The Overall Thermal Transfer Value (OTTV) is currently used by building designers to benchmark energy efficiency of building envelopes for commercial developments [2], whereas its validity is still arguable as its impact can be attributed to more elementary passive architectural design factors [3]. Passive design factors including the building layout, envelope design, geometry and air-tightness have been validated as effective energy conservation strategies by multiple sensitivity and optimization studies [4].

Most design optimization studies focus on envelope parameters under a fixed building size and outline. A box-shape low-rise building was optimized with PSO by varying the window size, overhang specifications and envelope thermal properties in four major climates of Iran, where energy performance of mono-criterion and multi-criterion approaches was compared [5]. A similar study investigated the optimal window size, orientation and wall reflectance configuration for a simple-box model considering different interior daylight indicators [6]. Harmathy et al. combined BIM (Building information modelling) with energy modelling engines and investigated the influence of window sizes and shapes on the indoor illumination quality and annual energy demand of a typical square-plan office building [7]. However, there are few optimization studies which considered the influence of different building shape and layout designs. The thermal and daylight performance of a typical school building was optimized with different dimensions and layouts of classrooms and corridors [8]. A 3D graphic software tool was coupled with EnergyPlus to vary the building space types. Each space type showed unique preference over optimal design parameters when the energy demand, thermal

comfort and daylight performance were taken as design objectives. The variation of the whole building form is however not included in this study. The shape coefficient, defined as the ratio of the external surface area of the air-conditioned building space to its inner volume, is then introduced as a key passive design factor in the building optimization. The simultaneous optimization of the shape coefficient, space efficiency and solar gain of the envelope was conducted on a free-shape building in severe cold areas of China [9]. The modelling concentrated on space dimension coordinates but ignored other common passive design factors and building operation conditions so that it can provide little practical indication of improving the energy and indoor environment performance. A proxy zone model with flexible folded facades was optimized through the combination of an hourly quasi-steady-state energy model and Radiance [10]. The research emphasized the effect of self-shading façade designs on the building energy, daylight and economic performance, but again failed to consider the potential impact of other architectural design strategies. A.L.S. Chan also studied the self-shading effect of different building shapes and flat layouts on the internal cooling load [11]. Further investigations on the natural ventilation and daylight performance by considering other architectural design factors were highly recommended in his future work plan. Regression analyses between the shape coefficient and window to wall ratio were conducted for a single-zone south-facing timber-glass building, where a strong linear correlation between the shape coefficient and total cooling and heating load was observed for cold regions [12]. Building shapes, shading specifications and window to wall ratios are optimized for a three-story medium office building to improve the energy and daylight performance [13]. In this study, the urban context is also presented in the modelling experiment to address shading effects from peripheral buildings, but design parameters are limited to discrete distributions.

The urban context is usually identified as a confounding factor, which cannot be controlled by building designers but can potentially impact the building performance. A fixed grid of rectangular peripheral building blocks with uniform intervals was considered in optimizing the window geometry, location, thermal and optical property of an office building to minimize the lighting, cooling and heating demand [14]. The variation of other envelope design parameters and diverse urban contexts were not addressed in this research. A similar study also conducted sensitivity analyses on building geometry designs with simplified urban contexts, where the building height, width, depth, distance

between buildings, floor area ratio, plot ratio, shape coefficient, verticality, aspect ratio and surface reflectance were changed in the modelling experiment [15]. The distance between buildings, aspect ratio (i.e. the ratio of the building heights to the distance between them) and surface reflectance were validated as the most influential factors when the obtained solar irradiance on building surfaces was the major concern. The effect of the reflectance and shading was summarized under the concept of Inter-Building Effect (IBE) in a sensitivity study on energy consumption within a building network [16]. This study also validated that a nine-building network was a simplified but reasonably robust modelling approach to study the impact of IBE. Reflectance, window to wall ratio and heat island effect of urban densification were also investigated for a Brazilian city in a hot and humid climate [17]. Only cooling loads of two office design layouts were studied and the shading effect was identified to have a major impact on load reduction. Allegrini et al. also investigated the impact of existing urban canyons on the prediction of building cooling demands [18]. Different street canyon configurations and corresponding shading control strategies were subject to sensitivity analyses to minimize the longwave radiation exchange between buildings. Apart from influence on indoor thermal environment, the effect of the building/ground surface albedo on the urban heat island index was evaluated by an outdoor thermal comfort indicator. The caused temperature rise in urban environment can influence the indoor climate in return [19]. Moreover, under a realistic urban context of New York, parametric analyses of residential buildings were carried out for passive architectural design factors with three typical plan shapes of the same floor area [20]. As another important confounding factor, the internal plug load (i.e. equipment power) in building operation was identified to be insignificant in the sensitivity analysis with two different power levels [20]. However, internal loads (heat gain) should also include lighting loads and occupant loads which can jointly contribute to a major part of the cooling load especially in a moderate climate such as UK [21]. Therefore, more studies related to the impact of the internal load should be conducted to reveal its actual influence over building sensitivity and optimization studies.

Based on the above introduction and literature review, most existing studies concentrate on a limited number or distribution of passive architectural parameters, while the potential impact of different archetypes and confounding factors on the design optimization process has not been sufficiently addressed. Especially, the impact of peripheral urban environment is usually limited to

building thermal performances without considering other important indicators such as the lighting demand and solar power generation potential. The uncertainty of sensitivity indices to archetypes and confounding factors are also scarcely addressed for promoting the robustness of statistical interpretation in diverse building design and operation scenarios. To fill such research gaps, this study proposed a holistic design optimization method to explore the design preference and energy conservation potential of office buildings with integrated photovoltaic (PV) envelope systems. The original contribution of this work lies in the following aspects: (1) The optimization of thermal and optical properties of PV facades are integrated with conventional passive architectural design factors, while maximum energy conservation potential under diverse building design and urban context scenarios are determined; (2) In-depth comparative modelling experiments are conducted to illustrate the impact of the shape coefficient, floor plan size, urban context and internal heat gain on sensitivity indices for main design factors by simultaneously considering the lighting, HVAC and power generation performance; (3) The shape coefficient is identified as the underlying key design factor for varied building geometries and floor sizes, and its linear correlation with building thermal demands is determined from parametric analyses. (4) The design optimization process is deeply coupled with local building energy and green building assessment codes, so that the main research finding is useful for upgrading commercial building benchmarks and facilitating decision-making process in green constructions.

## **2. Research design and methodology**

In this research, an EnergyPlus baseline model is first constructed with reference to local studies on commercial buildings and ASHRAE90.1 medium office prototypes [22-24]. Both independent passive architectural design variables and dependent PV envelope properties are identified as input variables to generate Monte Carlo sampling matrices. Modelling experiments are separately designed for different archetypes and confounding factors to perform both qualitative and quantitative sensitivity analyses. Design dimensions are thereafter reduced by bootstrapped sensitivity indices to conduct the high-efficiency hybrid generalized pattern search particle swarm optimization (HGSPSO). Optimum design solutions and design parameter weightings for each archetype and confounding factor are subject to in-depth comparative analyses based on lighting, HVAC and power

generation indicators. The overall research framework is summarized in Fig. 1 and detailed explanations are made in the following subsections (i.e. Section 2.1 to 2.3).

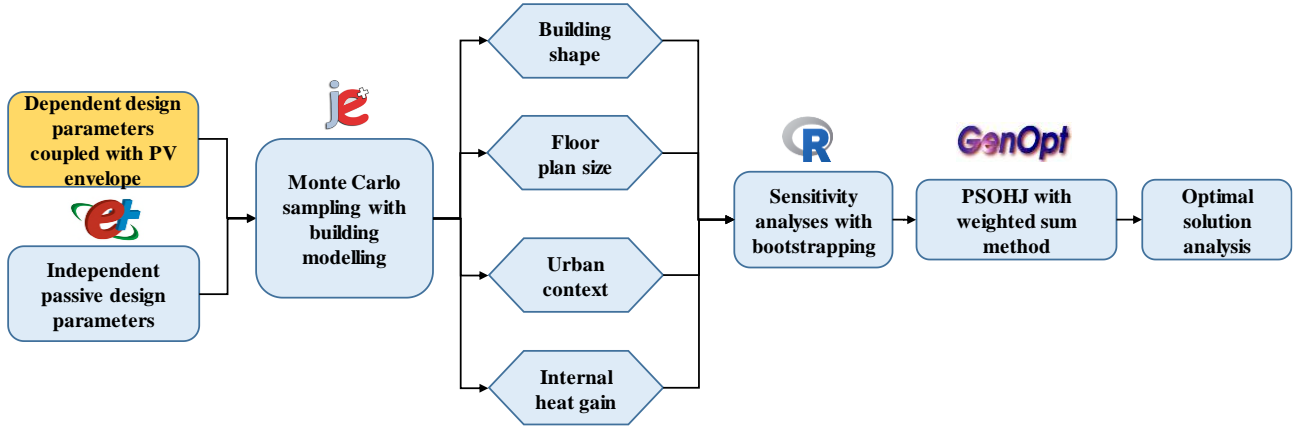


Fig. 1. Proposed research design framework

## 2.1. Setting of baseline model and input variable

The baseline building model is first constructed in SketchUp and imported to EnergyPlus to represent a typical high-rise office building in Hong Kong. Important passive architectural design factors are selected as input for modelling experiments while their interactions with PV envelope parameters are specified in this section.

### 2.1.1. Selecting input variable

Passive architectural design parameters for a typical office building mainly consist of two categories: independent variables and dependent variables. The building orientation (BO), window visible transmittance (VT), window U-value (WU), Infiltration air change per hour (IACH), wall thermal resistance (WTR), wall specific heat (WSH), overhang projection fraction (OPF), window to wall ratio (WWR) and light to solar gain ratio (LSG) are all basic design elements identified from previous research for high-rise residential buildings, in which their collinearity has been eliminated by calculated variance inflation factors (VIF) [25]. These key passive design parameters are chosen based on screening-based and sampling-based sensitivity studies. Especially, window to ground ratio (WGR) is replaced by WWR in this study because no compulsory regulation is imposed on WGR for commercial developments in Hong Kong. On top of the above independent variables, the solar heat gain coefficient (SHGC), active glazing PV area (GPVA) and active wall PV area (WPVA) are

identified as dependent variables to integrate PV facades with traditional passive architectural design variables. WPVA is determined as 90% of the opaque wall area which covariates with the window to wall ratio once the space geometry is fixed. SHGC and GPVA are defined by Eq. (1) and (2) in Table 1. The distribution range of LSG reflects the changing thermal/optical properties from single-pane clear glazing to spectrum-selective insulative glazing [26]. The coefficient of 0.9 in Eq. (2) is under the assumption that the semi-transparent PV window is composed of opaque solar cells and glazing with 90% transparency.

Table 1. Specification of input variables

Design parameter	Value range	Baseline value	Distribution
BO (°)	0~180°	0	Uniform, Continuous
WSH (J/kg·K)	800~2000	840	Uniform, Continuous
VT	0.24~0.9	0.786	Uniform, Continuous
WTR (m <sup>2</sup> ·K/W)	0.09~6.25	0.136	Uniform, Continuous
LSG	1.0~2.4	1.118	Uniform, Continuous
WWR	0.1~0.8	0.833	Uniform, Continuous
WU (W/m <sup>2</sup> ·K)	0.2~6	2.63	Uniform, Continuous
OPF	0.0~0.6	0.0	Uniform, Continuous
IACH (h <sup>-1</sup> )	0.05~1.5	0.6	Uniform, Continuous
SHGC	$SHGC = \frac{VT}{LSG} = \tau + \alpha p$	(1)	Uniform, Continuous
GPVA	$GPVA = 1 - \frac{VT}{0.9}$	(2)	Uniform, Continuous

Note:  $\tau$  is the directly transmitted solar radiation through the window;  $\alpha$  is the absorbed solar radiation by the window panel; and  $p$  is the proportion of absorbed solar radiation which is eventually transferred to the indoor ambience.

### 2.1.2. Building baseline model

High-rise buildings are common archetypes in the commercial sector of densified urban areas such as New York, Tokyo, Beijing and Hong Kong. Hong Kong is selected as the representative of the hot and humid climate with abundant solar radiation where both PV and passive design technologies have great application potential. The weather profile in the format of IWEC (International Weather for Energy Calculations) developed by City University of Hong Kong is used as the model input to assess the annual building energy performance. A 40-story office building with a typical floor plan as per Fig. 2 is divided to five thermal zones: North zone, East Zone, South Zone, West Zone and Core Zone. The typical floor has a dimension of 36m (Length) \* 36m (Width) \* 3m (Height), with a perimeter zone depth of 4.6m [20, 24]. The window to wall ratio is set to be 83.33%

to indicate a common curtain wall scenario in Hong Kong.

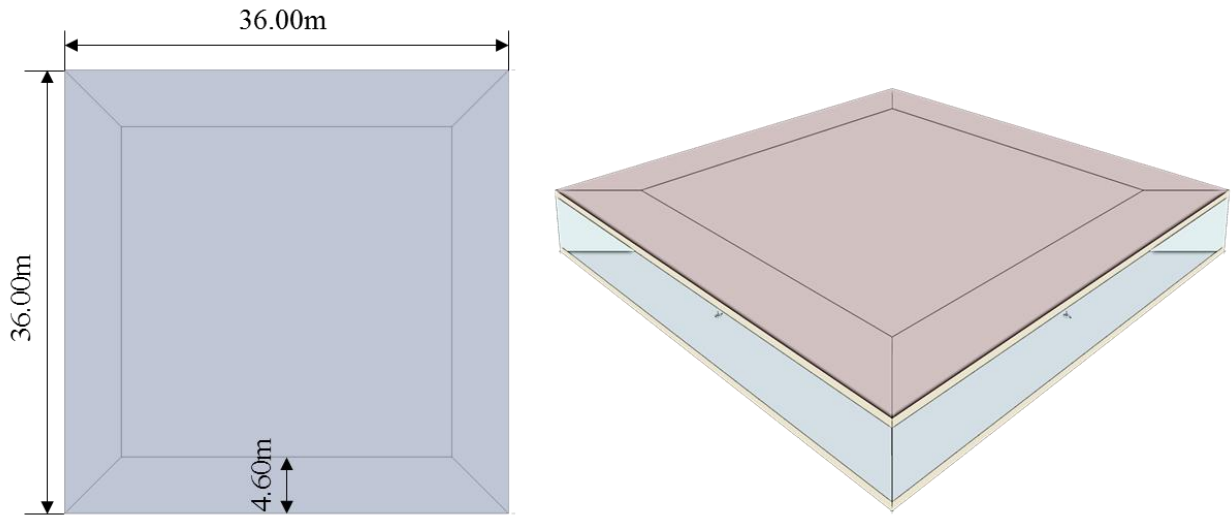


Fig. 2. Baseline model layout plan

Table 2. Miscellaneous settings of the baseline model

Item	Setting	Schedule
Occupancy Activity level	8 m <sup>2</sup> /person 120 W/person	All days: (0:00-6:00: 0.0, 6:00-7:00: 0.1, 7:00-08:00: 0.2, 8:00-12:00: 0.95, 12:00-13:00: 0.5, 13:00-17:00: 0.95, 17:00-18:00: 0.3, 18:00-20:00: 0.1, 20:00-24:00: 0.05)
Lighting gain Illuminance setpoint	12 W/m <sup>2</sup> 300 Lux	All days: (0:00-5:00: 0.05, 5:00-7:00: 0.1, 7:00-8:00: 0.3, 8:00-17:00: 0.9, 17:00-18:00: 0.5, 18:00-20:00: 0.3, 20:00-22:00: 0.2, 22:00-23:00: 0.1, 23:00-24:00: 0.05)
Equipment gain	10 W/m <sup>2</sup>	All days: (0:00-8:00: 0.4, 8:00-12:00: 0.9, 12:00-13:00: 0.8, 13:00-17:00: 0.9, 17:00-18:00: 0.5, 18:00-24:00: 0.4)
HVAC system	IdeaLoadsAirSystem	-
Cooling Setpoint	24/30 °C (Setback)	-
Heating Setpoint	21/15 °C (Setback)	-
Outdoor air flow	0.008 m <sup>3</sup> /s·person	-
PV conversion efficiency	Monocrystalline silicon: 15% Amorphous silicon: 6.3%	-

The baseline model is constructed without urban contexts in EnergyPlus, which is a valid



simulation platform for predicting the daylight, thermal and energy performance of buildings [27-29]. The platform incorporates shading, daylight, air/thermal balance submodules with photovoltaic generators to provide energy demand indicators for sensitivity and optimization studies. Miscellaneous internal loads (heat gain) and building operation schedules for the baseline case are specified in Table 2 with reference to ANSI/ASHRAE/IES Standard 90.1 and local building energy codes [30, 31]. A simplified ideal HVAC system model was adopted to meet the indoor cooling/heating loads with an overall energy conversion efficiency of 1.0. Dimming controls are turned off for the baseline model but are activated for design cases to maintain the illumination setpoint with natural and artificial lighting. One reference daylight sensor in the center of each perimeter zone at the height of 0.85m is used to modulate the lighting power consumption. The Simple generator model is coupled with both opaque and transparent building facades to preliminarily predict power generation assuming an average conversion efficiency of 6.3% for semi-transparent amorphous silicon and 15% for opaque monocrystalline silicon modules [32-34]. All building services system and control strategies are kept constant to maintain the focus on selected key design parameters.

## **2.2.Determining archetypes and confounding factors**

This section specifies the setting of four main scenarios of modelling experiment: the building shape, floor plan size, urban context and internal load (heat gain), which are classified as building archetypes and confounding factors as below.

### **2.2.1. Variation of building archetypes**

Building archetypes are varied by modulating the size and shape of the typical floor plan for a high-rise commercial building. The baseline floor plan of 36\*36m corresponds to a medium office as per commercial building prototypes developed by U.S. Department of Energy (DOE). Consequently, the small and large office prototype models were also adapted according to Hong Kong's building energy codes to represent diverse floor sizes in comparative modelling experiments. Fig. 3 illustrates a small office plan of 24\*24m and a large office plan of 48\*48m in addition to the baseline case. Currently, commercial prototype buildings in U.S. can cover 80% of newly constructed commercial

floor areas, but no such model has been developed in Hong Kong. This research will also examine the applicability of these adapted models in local building sectors.

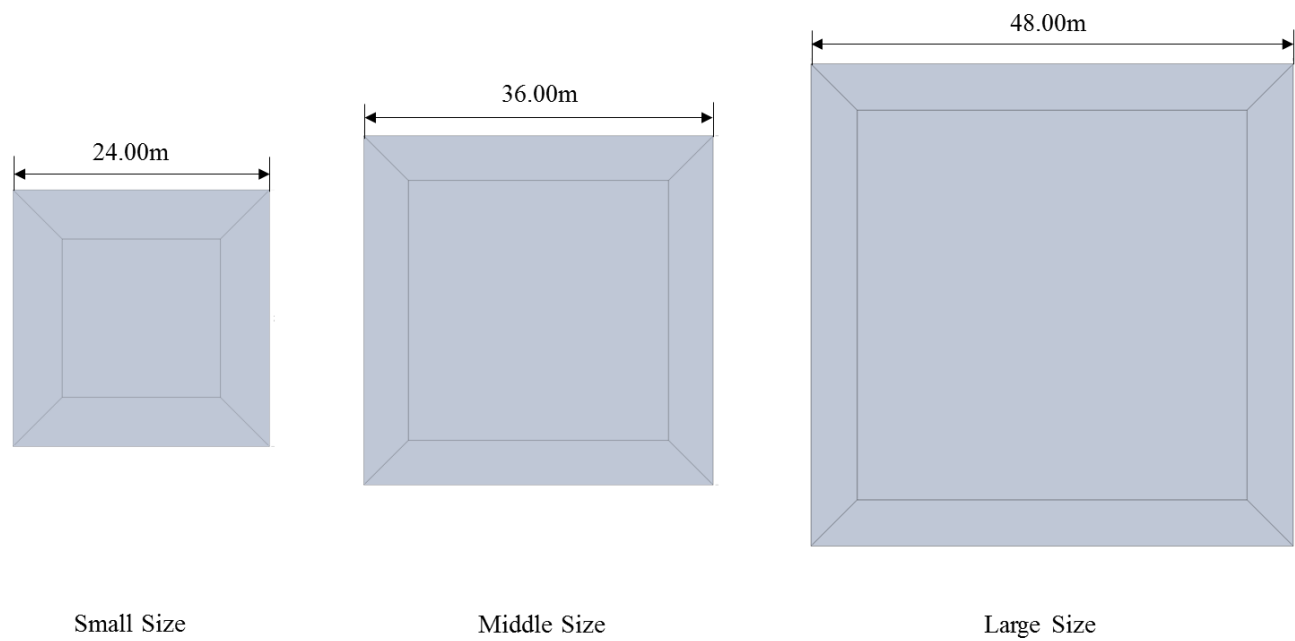


Fig. 3. Variation of the plan size for typical office floor

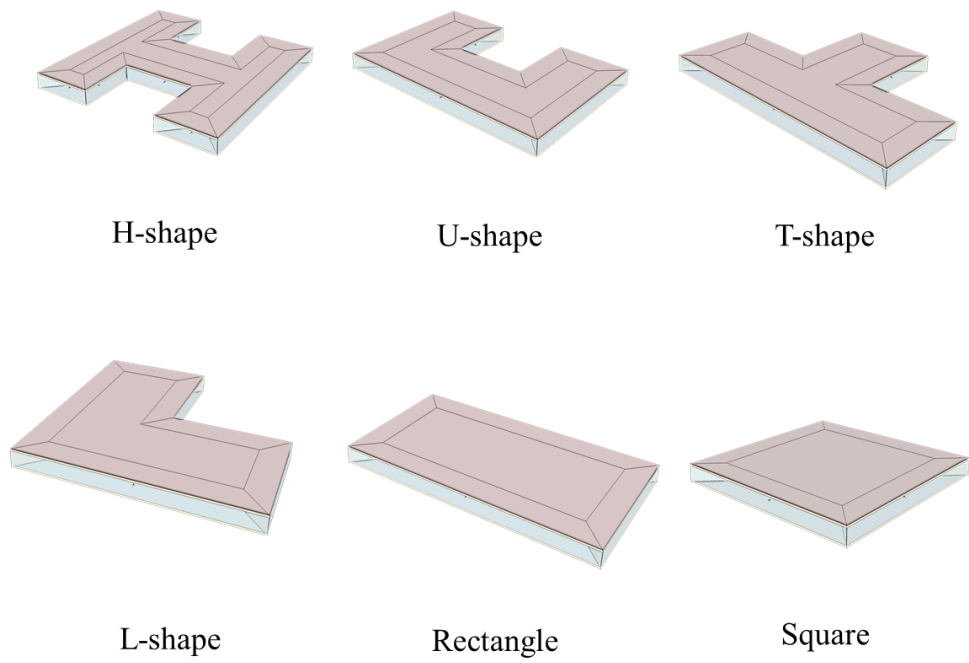


Fig. 4. Variation of the plan shape for typical office floor

In addition to the variation of plan size, the diversity of building morphology is further explored with five other common plan shapes: Rectangle, L-shape, T-shape, U-shape and H-shape (See Fig. 4). All five layout plans have the same floor area as the baseline model and symmetric wings to the building central line. The rectangle shape has an aspect ratio (i.e. building length/width) of 1.92:1 compared to 1:1 for the square shape. L-shape, T-shape, U-shape and H-shape buildings are subject to self-shading effects and the envelope area is apparently increased compared to Square and Rectangle plans. Such variation leads to different shape coefficients (SC) as defined by the ratio between the external surface area of the air-conditioned building space and its inner volume. For a high-rise building with relatively small roof areas, the shape coefficient can be approximated by the ratio of the vertical façade area to the total space volume. The perimeter zone depth for each layout plan is maintained as 4.6m [20].

#### 2.2.2. Variation of confounding factors

Confounding factors are defined as variables that have potential influence over the design optimization decisions but can barely be controlled by the design team [20]. The density of urban context is one of these confounding factors that is proved to have potential influence on building thermal and daylight performances [18, 35]. Building designers have, however, minor control over the site selection and peripheral condition in a new development or especially a renovation of the existing development. In most green building assessment schemes such as BEAM Plus and LEED, urban contexts related criteria are usually assessed in the site aspect/category, whereas stand-alone buildings are simulated in the energy or indoor environment aspects/categories. This assessment approach should be improved by integrating the urban context into the whole building simulation to sufficiently address shading/reflection from the peripheral environment.

Office buildings in Hong Kong mainly assemble in Hong Kong Island and Kowloon, while some are scattered in the broad New Territory. As shown in Fig. 5, Central, Mongkok and Shatin are selected as three representative commercial sectors for high-density, medium-density and low-density urban contexts. The high-density context is defined as the neighbourhood with an average building height of 120m (i.e. about 40 floors) and a building height to the street width ratio (H/W) of 12:1. The medium-density context is defined as the neighbourhood with an average building height of 75m (i.e.

about 25 floors) and an H/W of 3.75:1. The low-density context is defined as the neighbourhood with an average building height of 30m (i.e. about 10 floors) and an H/W of 1:1. The three urban context scenarios are simplified to building matrices in Fig. 6.



Fig. 5. Selected commercial sectors within Hong Kong

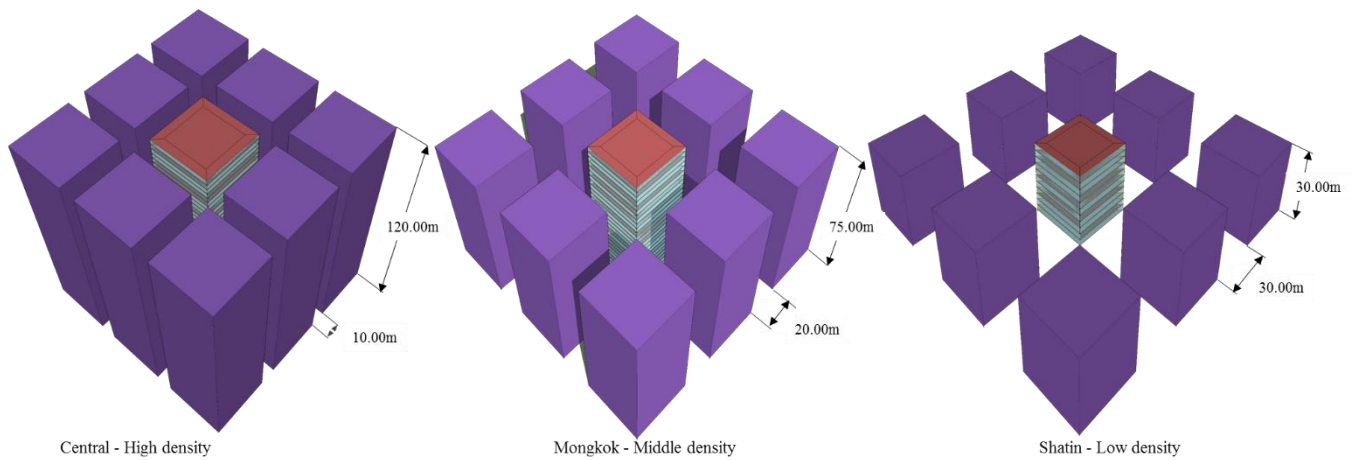


Fig. 6. Real urban contexts and corresponding modelling cases

The simplification of urban contexts is necessary because too many shadow overlaps might extensively slow down the process of a modelling experiment with thousands of running cases. Adopting reduced peripheral shading dimensions by unifying building heights/shapes and excluding non-effective shading surfaces has been proved to be a feasible approach to improve computation efficiency while generate consistent trends with real-context simulations [16, 36, 37].

Another confounding factor identified from existing literatures is the internal heat gain (internal load) [20, 21]. Plug loads (including the lighting and small power) were found to significantly affect

the indoor temperature and corresponding cooling/heating demands, but not obviously change the design preference. In this study, not only plug loads but also the occupant heat gain is included in the modelling experiments to further explore the impact of the total internal load. Three levels of internal loads are examined as per Table 3: a baseline (medium) level according to the Building Energy Code of EMSD; a low level reduced to half of the baseline to indicate the energy-saving appliance and low space occupancy [21]; a high level doubling the baseline to indicate the high end-use intensity and space occupancy.

Table 3. Summary of the internal load in different levels

Item	Low level	Medium level	High level
Occupancy gain	16 m <sup>2</sup> /person 120 W/person	8 m <sup>2</sup> /person 120 W/person	4 m <sup>2</sup> /person 120 W/person
Lighting gain	6 W/m <sup>2</sup>	12 W/m <sup>2</sup>	24 W/m <sup>2</sup>
Equipment gain	5 W/m <sup>2</sup>	10 W/m <sup>2</sup>	20 W/m <sup>2</sup>
Peak internal gain	18.5 W/m <sup>2</sup>	37 W/m <sup>2</sup>	74 W/m <sup>2</sup>

### 2.3. Performing holistic building design optimization

A holistic building design optimization is proposed by incorporating sensitivity analyses with the hybrid particle swarm optimization algorithm in a joint modelling platform of JEPlus, R and GenOpt. Because non-linearity and non-additivity have been identified by the correlation test conducted on passive architectural design parameters [38, 39], Morris and FAST (Fourier Amplitude Sensitivity Test) are adopted as two appropriate sensitivity analysis approaches to obtain qualitative and quantitative factor prioritizing results. Bootstrapping is then applied with R packages to assess the uncertainty of FAST total-order indices for factor fixing and reducing the dimension of further optimization problems.

The Morris method is adopted to qualify the sensitivity of building energy demands to each design parameter with a limited sample size of  $r(k+1)$ , where  $r$  is the number of trajectories and  $k$  is the dimension of input parameters. In this method, the significance of each input variable is measured by statistics of the Elementary Effect (i.e.  $EE_i$ ) [40], where the absolute mean  $\mu^*$  shows the main effect of each design input and the standard deviation  $\sigma$  shows the non-linearity and parametric interactions [40]:

$$\mu^* = \sum_{i=1}^r |EE_i| / r \quad (3)$$

$$\sigma = \sqrt{\sum_{i=1}^r (EE_i - \mu)^2 / r} \quad (4)$$

The FAST method is then used to quantify the obtained preliminary sensitivity indices from Morris. The total variance of the model output (i.e. energy demands) is decomposed to the unique impact of each design input ( $V_i$ ) and the joint impact of two or more design inputs ( $V_{12...k}$ ). The first-order sensitivity index ( $S_i$ ) is then derived for factor prioritizing and the total-order index ( $S_{Ti}$ ) is derived for factor fixing. In this approach, a multi-dimensional transformation of input space (from  $x_i$  to a scalar  $-\infty < s < +\infty$ ) is conducted and the minimum required number of model evaluations is determined by Eq. (5) and (6):

$$x_i = \frac{1}{2} + \frac{1}{\pi} \arcsin(\sin(\omega_i s + \varphi_i)) \quad (5)$$

$$N = 2M\omega_{\max} + 1 \quad (6)$$

where  $M$  (usually set to 4) is the number of harmonics to sum in the Fourier series decomposition (i.e. the interference factor);  $\omega_{\max}$  is the maximum value among frequencies  $\omega_i$  [41, 42]. Furthermore, bootstrapping of FAST total-order indices is conducted with R packages to evaluate their uncertainties and consolidate factor fixing results [25].

The global optimization of significant design inputs identified from sensitivity analyses is further conducted to explore the energy conservation potential of high-rise office buildings in different design scenarios. The lighting demand, HVAC demand and PV energy supply are summarized as the net building energy demand with the weighted sum method, which turns the multivariate optimization to the univariate optimization [43].

Although there are many optimization algorithms applicable to non-linear energy and building systems [44, 45], the hybrid generalized pattern search particle swarm optimization (HGPPSO) in GenOpt is adopted to solve the univariate optimization problem by evaluating and updating modelling results in EnergyPlus given its high efficiency and availability [46]. GenOpt is a generic optimization program developed by Lawrence Berkeley National Laboratory. It can be coupled with EnergyPlus by setting the command file, configuration file and initialization file. In command files, variation of input parameters as well as optimization and algorithm settings are specified. The configuration file

sets the location of simulation engines, error messages and the way to read and write simulation files. The initialization file summarizes objective functions for evaluation and locations of all necessary files. All details of the program can be found in its user manual and the algorithm section of the GenOpt command file is illustrated as per Table 4.

Table 4 The algorithm section of HGPSPSO with Hooke-Jeeves (i.e. GPSPSOCCHJ)

Algorithm {	
Main	= GPSPSOCCHJ
NeighborhoodTopology	= gbest   lbest   vonNeumann
NeighborhoodSize	= 5
NumberOfParticle	= 10
NumberOfGeneration	= 10
CognitiveAcceleration	= 2.8
SocialAcceleration	= 1.3
MaxVelocityGainContinuous	= 0.5
MaxVelocityDiscrete	= 4
ConstrictionGain	= 0.5
MeshSizeDivider	= 2
InitialMeshSizeExponent	= 0
MeshSizeExponentIncrement	= 1
NumberOfStepReduction	= 4
}	

In the first stage of HGPSPSO, the particle swarm optimization (PSO) is operated by emulating the food searching behavior of bird flocks, in which each particle/individual acts in a certain rule leading to a collective high-performance cooperation [47]. The individual best solution obtained by a particle is compared with the global best solution by all particles in each generation for updating its velocity and position in the next generation. GenOpt improved PSO's capability in finding global optima by introducing a constriction coefficient  $\chi(\kappa, \varphi)$  to expedite the convergence process and improve the exploitation as per Eq. (7) and (8):

$$v_i(t+1) = \chi(\kappa, \varphi)v_i(t) + c_1\rho_1(t)(p_{l,i}(t) - x_i(t)) + c_2\rho_2(t)(p_{g,i}(t) - x_i(t)) \quad (7)$$

$$\chi(\kappa, \varphi) \triangleq \begin{cases} \frac{2\kappa}{2 - \varphi\sqrt{\varphi^2 - 4\varphi}}, & \text{if } \varphi > 4 \\ \kappa, & \text{otherwise} \end{cases} \quad (8)$$

where  $t$  is the number of generations;  $x_i(t)$  is the  $i^{th}$  particle's position in  $t^{th}$  generation;  $p_{l,i}(t)$  is the position where  $i^{th}$  particle yield the best solution;  $p_{g,i}(t)$  is the position of the best particle over all

generations;  $c_1$  is the cognitive acceleration constant;  $c_2$  is the social acceleration constant;  $\rho_1(t)$  and  $\rho_2(t)$  are random numbers between 0 and 1 to prevent the concentration of particles in the search space and increase the diversity of solutions;  $\varphi \Delta c_1 + c_2$  and  $\kappa \in (0,1]$  are speed controllers by which the population collapses to one point.

Based on the solution obtained from PSO, The Generalized Pattern Search (GPS) with Hooke-Jeeves is further applied to obtain derivative-free minimization in the optimization problem [46]. Stationary accumulation points and a mesh in the input domain are constructed and explored based on the distance reduction rule in the iterative progress. HGPSPSO can therefore increase both the optimization efficiency and accuracy compared with traditional PSO and GPS.

### 3. Results and discussions

This section elaborates the uncertainty of the sensitivity analysis and design optimization of high-rise commercial buildings under varied archetypes and confounding factors. The adapted commercial prototype model is validated by statistical summaries of office building energy consumption in Hong Kong. Passive architectural design preferences and their energy conservation potential are analyzed and discussed under different floor plan shapes, sizes, urban contexts and internal load (heat gain) levels.

#### 3.1. Benchmarking the baseline design

The high-rise office building is adapted from ASHRAE90.1 commercial prototype buildings representing 80% of typical floor areas in U.S. Although EnergyPlus has been tested and validated by extensive theoretical and experimental studies [13, 27], the adapted baseline model is still benchmarked with the statistical energy use data from the Hong Kong government. According to the latest Hong Kong Energy End-use Data, the whole office segment consumed 13182 TJ electricity in 2016 alone. Its average energy use index (per floor area) was estimated as 314.57 kWh/m<sup>2</sup> based on the statistics by Rating and Evaluation Department. The total energy use of lighting, HVAC and equipment should then be estimated as 254.51 kWh/m<sup>2</sup> referring to the breakdown of electricity consumption by end-uses [1]. The obtained energy use index also coincides with the statistical



average value obtained from a random sampling on Grade A offices in Hong Kong [48]. On the other side, the baseline model is simulated with the existence of high-density urban context in Hong Kong, and the energy use index is predicted to be 245.55 kWh/m<sup>2</sup> (i.e. 3.52% lower than the benchmark calculated from official statistics and literatures). The breakdown of total energy demand for both official statistics and the baseline simulation is shown in Fig. 7. From the consistence of end-use proportions and total energy demands, the baseline model with urban contexts can be used to represent the average office building performance in Hong Kong.

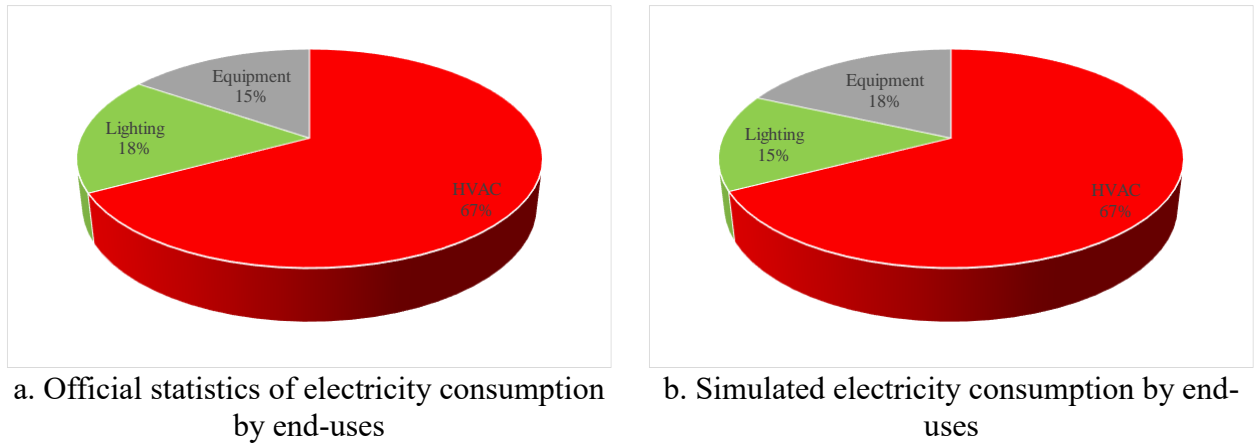


Fig. 7. Office energy use indices by end-uses

### 3.2. Design optimization for the reference case

The benchmarked baseline model is then modified by removing the urban context to represent the worst case with an annual energy demand of 304.21 kWh/m<sup>2</sup>. This is deemed as the reference case for further modelling experiments conducted with different archetypes and confounding factors. Morris indices based on 100 model evaluations and FAST first-order indices based on 5670 model evaluations are illustrated in Fig. 8 [40]. The  $\mu^*$  -  $\sigma$  chart in the left is divided to four zones by the line  $\sigma/\mu^*=0.1$ ,  $\sigma/\mu^*=0.5$ ,  $\sigma/\mu^*=1$ . Most of design parameters, including VT (visible transmittance), LSG (light to solar gain ratio), WU (window U-value), OPF (overhang projection fraction) and IACH (infiltration air change per hour), fall in the area between  $\sigma/\mu^*=0.5$  and  $\sigma/\mu^*=1$ , indicating an almost monotonic relationship with the net energy demand. WWR (window to wall ratio) falls in the area between  $\sigma/\mu^*=0.1$  and  $\sigma/\mu^*=5$ , indicating a monotonic relationship with the net energy demand. WTR (wall thermal resistance) falls in the area with  $\sigma/\mu^*>1$ , indicating a non-linear and non-monotonic relationship with the net energy demand. None of the design parameters falls in the area with  $\sigma/\mu^*<0.1$ ,

indicating the exclusion of the linear relationship with the net energy demand [49]. BO (building orientation) is however close to the zero point in the figure, indicating less importance and interactions with other parameters. The above analysis validated that the variance-based sensitivity approach is more appropriate than the traditional linear regression in this study. The ranking of passive design parameters and their correlations with the model output also achieved consistence with a previous study on a small-scale office [39].

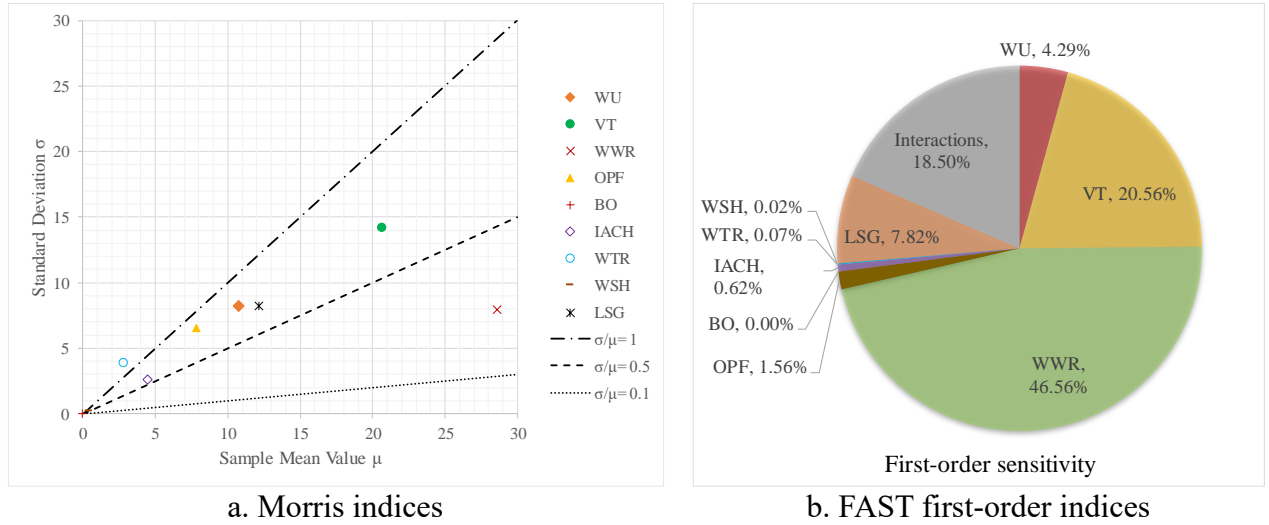


Fig. 8. Morris and FAST first-order indices for the integrated passive design and PV systems

Fig. 8b further quantifies the unique and joint influence of passive design parameters on the net energy demand. According to FAST first-order indices, WWR makes the highest contribution of 46.56% to the variation of the model output, because it can simultaneous affect the HVAC, lighting and PV energy performance. VT and LSG rank second and third given their contribution of 20.56% and 7.82% respectively. WU ranks after LSG with a noticeable contribution of 4.29%, while remaining design inputs make non-significant unique contributions. It is however noteworthy that interactions of all input variables account for 18.5% of the output variation, indicating that total-order indices involving interactive effects between design variables have to be obtained for factor fixing. In addition, the ranking of design parameters achieved complete consistence between Morris and FAST predictions which echo with existing statistical theories [40, 50]

FAST total-order indices and its uncertainties based on bootstrapping are then summarized in Table 5. The 95% confidence intervals for OPF, BO, IACH, WTR and WSH contain zero under

standard deviations between 0.020 and 0.021. These design parameters are then excluded from the optimization problem space as non-significant factors to be fixed at baseline levels. As a result, the holistic optimization of remaining four design factors leads to a minimized net building energy demand of 192.169 kWh/m<sup>2</sup> (i.e. 36.83% saving compared with the reference scenario) within 382 iterations. The energy-saving is mainly derived from the reduced lighting and HVAC consumption of 23.335 kWh/m<sup>2</sup> and 147.888 kWh/m<sup>2</sup> as well as an increased PV power generation of 26.424 kWh/m<sup>2</sup>. The optimum design is characterized by a high window heat transfer coefficient of 5.85 W/m<sup>2</sup>·K and light to solar gain ratio of 2.4 while low window to wall ratio of 10.01% and visible transmittance of 0.323.

Table 5 Bootstrapped FAST total-order indices for the integrated passive design and PV systems

	Original FAST total-order indices	Standard error	95% confidence interval lower	95% confidence interval upper
WU	0.067	0.021	0.027	0.108
VT	0.285	0.020	0.245	0.325
WWR	0.577	0.020	0.538	0.617
OPF	0.038	0.021	-0.002	0.079
BO	0.003	0.021	-0.039	0.043
IACH	0.011	0.020	-0.029	0.051
WTR	0.008	0.021	-0.033	0.048
WSH	0.003	0.020	-0.037	0.043
LSG	0.130	0.022	0.087	0.172

### 3.3. Impact of floor plan shapes

The impact of floor plan shape is investigated by comparing the design optimization results of the reference scenario with five other commonly adopted scenarios. Based on the comparison detailed in Fig. 9, factor prioritizing of high-rise office buildings is barely influenced by the variation of plan shapes and the corresponding difference in facade areas and self-shading conditions. The ranking of significant design factors maintains constant while their exact contribution to the net energy demand fluctuates within 1%.

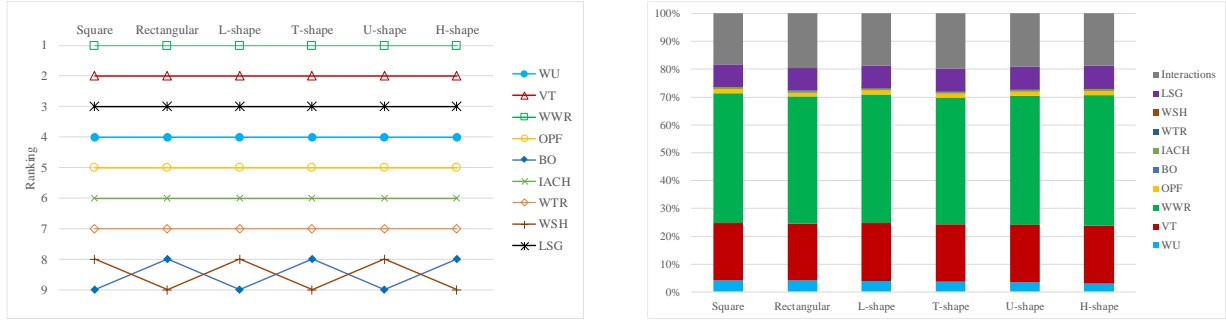


Fig. 9. Impact of building shape on factor prioritizing

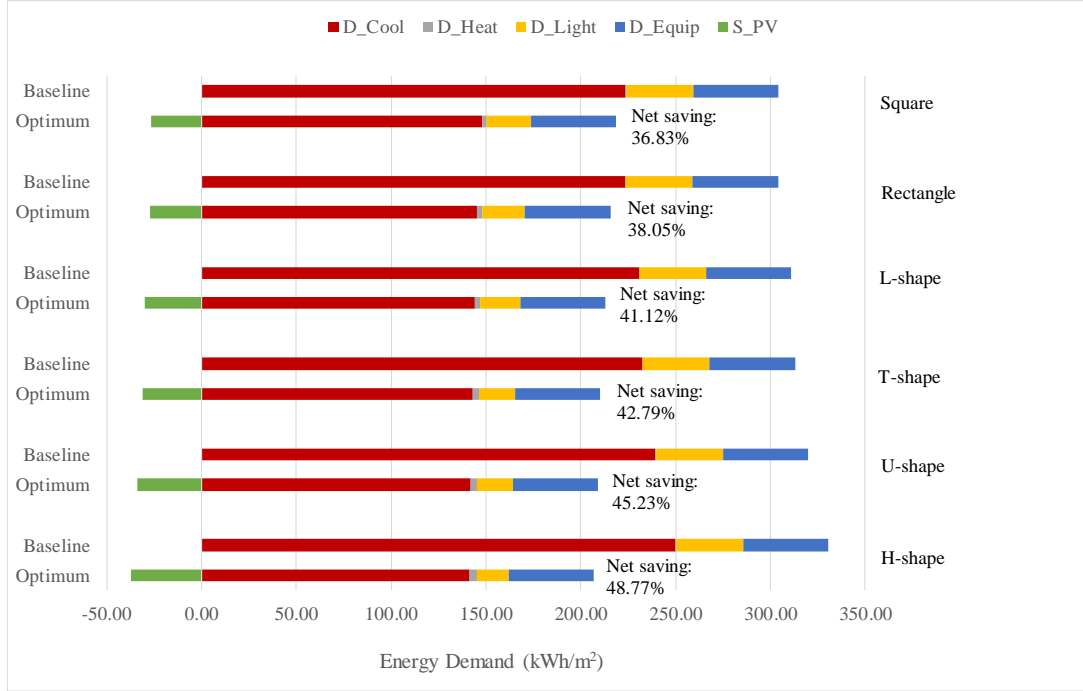


Fig. 10. Comparison of baseline and design energy performances of different building shapes

On the contrary, optimization results and energy performances of both baseline and optimum scenarios are heavily influenced by building shapes. As shown in Fig. 10, the net energy-saving potential compared with baseline designs increases from 36.83% of the square shape to 48.77% of the H-shape. Meanwhile, the building shape coefficient (SC) also increases from 0.11 of the square shape to 0.16 of H-shape. Lighting and equipment energy demands maintain constant for all baseline designs, while lighting demands of optimum designs vary between 23.335 and 16.327 kWh/m<sup>2</sup> by up to 30.03% with different shape coefficients. HVAC energy demands (i.e. the sum of cooling and heating) of baseline designs vary in a broad range between 223.724 and 250.198 kWh/m<sup>2</sup>, whereas those of optimum designs fluctuate slightly within 3.42% between 145.244 and 150.388 kWh/m<sup>2</sup>. A larger SC should have both negative and positive impact on thermal loads because of the coexistence

of enlarged external surface areas and self-shading effects. In this modelling experiment, the negative impact apparently dominated given the increased baseline HVAC demands. On the supply side, the PV power generation of optimum designs varies from 26.424 to 37.324 kWh/m<sup>2</sup> by up to 41.25%. Among optimum solutions, all shape design scenarios prefer a small window to wall ratio (WWR) around 10% and a high light to solar gain ratio (LSG) of 2.4. However, square, rectangle, and L-shape buildings prefer a relatively lower visible light transmittance (VT) between 0.319 and 0.366 as well as a relatively higher WU between 5.763 W/m<sup>2</sup>·K and 5.850 W/m<sup>2</sup>·K compared with other shape designs. The above changes in design preferences are summarized in Table 6.

Table 6. Optimum design solutions for different plan shapes

	SC -	D_Light (kWh/m <sup>2</sup> )	D_HVAC (kWh/m <sup>2</sup> )	S_PV (kWh/m <sup>2</sup> )	WU (W/m <sup>2</sup> ·K)	VT -	WWR -	LSG -
H-shape	0.16	16.327	145.360	37.324	3.400	0.661	0.10	2.4
U-shape	0.15	19.014	145.244	33.874	3.431	0.435	0.10	2.4
T-shape	0.14	19.274	146.123	31.303	3.400	0.661	0.10	2.4
L-shape	0.13	21.389	146.841	29.903	5.850	0.366	0.10	2.4
Rectangle	0.12	22.617	147.945	27.204	5.763	0.319	0.10	2.4
Square	0.11	23.335	150.388	26.424	5.850	0.323	0.10	2.4

Note: Lighting energy demand - D\_Light; HVAC energy demand - D\_HVAC; PV energy supply - S\_PV

Among above variation in baseline and design scenarios, HVAC energy demands of baseline designs are approximately linearly correlated with their corresponding shape coefficients as per Fig. 11. The regression model achieved a high value of 0.9588 for the coefficient of determination (i.e. R<sup>2</sup>), indicating that fitted model can account for most of the variation in the net building energy demand. Yang et al. obtained such an ideal correlation between the shape coefficient and heating demand, but the heating demand is calculated with a simplified building load coefficient without considering the envelope thermal capacity and internal heat gain [51]. Premrov et al. also correlated the shape factor with the building thermal load but the fitted linear regression equations had a much lower inclination between 22.356 and 44.322 [12]. The difference in the inclination might result from

the difference in scales and configurations of simulated layout plans. In their research, hypothetical single-sided generic models (i.e. all windows were placed on the south façade) with shape factors between 1.47 and 1.72 were simulated, whereas the average building shape coefficient is around 0.16 for the realistic whole-scale building this research [23]. Therefore, the fitted regression equation in Fig. 11 should be a more meaningful guide to the building performance optimization in the local industry.

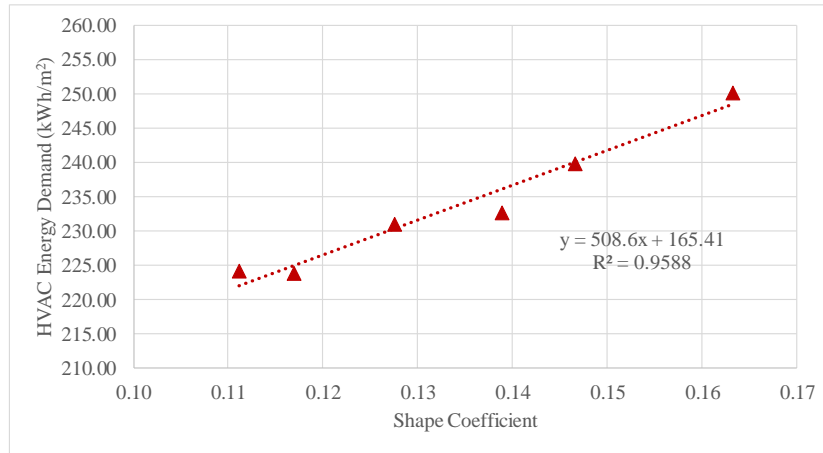


Fig. 11. Correlation between shape coefficients and HVAC energy demands

The shape coefficient also affects the lighting energy demand and PV power supply, which are scarcely mentioned in existing literatures. Fig. 12 presents the variation of the lighting energy demand for optimum solutions with respect to the shape coefficient and visible transmittance. The lighting energy is generally inversely correlated with the shape coefficient, while when SC is fixed the lighting demand slightly decreases with increased VT. Architectural designs with larger SC have both positive and negative impact on the lighting performance with enlarged perimeter zones and increased self-shading. The positive impact again dominated for the lighting demand in this study. On the contrary, the PV energy supply generally increases with SC as illustrated in Fig. 13. When SC is fixed to a certain value, the power generation can be either increased or decreased slightly with VT, indicating a trade-off between the self-shading effect and increased glazing PV area (correlated with VT as per Eq. (2)).

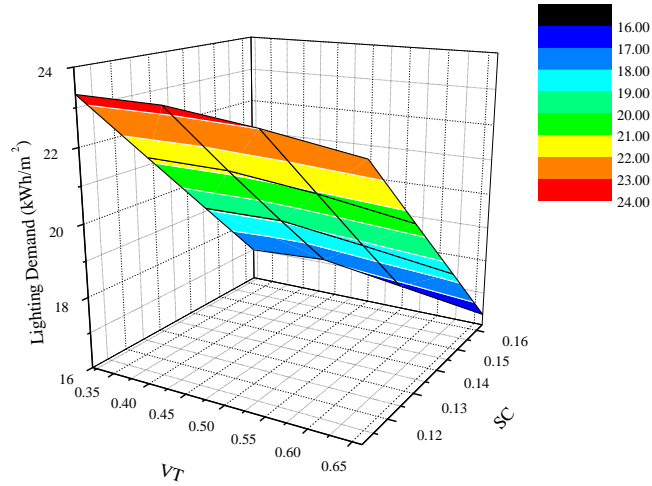


Fig. 12. Variation of lighting demands with shape coefficients and visible transmittance

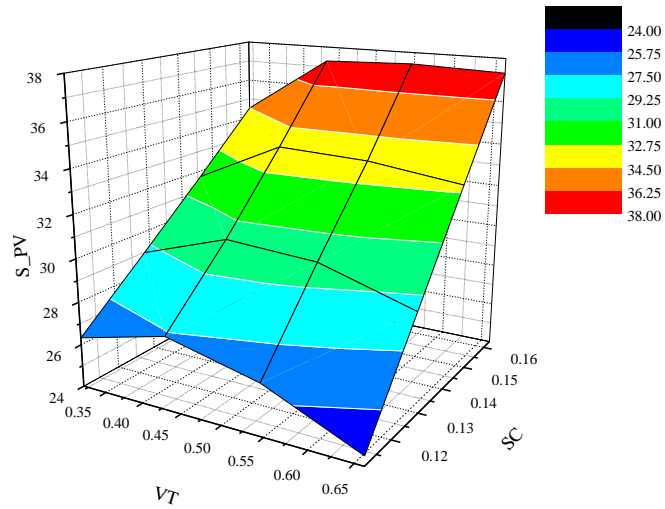


Fig. 13. Variation of PV energy supplies with shape coefficients and visible transmittance

### 3.4. Impact of floor plan sizes

Similar to varying the floor shapes, the floor size has a minor influence over the factor prioritizing result as shown in Fig. 14. The ranking of all design parameters is kept constant, while the exact contribution of each design input varies within 3%. However, the optimization potential and energy performances of both baseline and optimum scenarios are greatly influenced by plan sizes. As shown in Fig. 15, the net energy-saving potential compared with baseline designs increases from 29.66 to 48.53% with decreased floor sizes. Lighting and equipment energy demands maintain constant for all baseline designs, while the lighting demand of optimum designs varies between 19.005 and 25.926 kWh/m<sup>2</sup> by up to 36.42% with different floor plan sizes. HVAC energy demands of baseline designs vary in a broad range between 211.906 and 251.202 kWh/m<sup>2</sup>, whereas those of

optimum designs fluctuate slightly within 5.64% between 146.217 and 154.465 kWh/m<sup>2</sup>. On the supply side, the PV power generation of optimum designs varies from 19.837 to 39.562 kWh/m<sup>2</sup> by up to 49.86%. In terms of the design space for optimum solutions, all building designs prefer a small WWR around 10%, a high LSG of 2.4 and a low VT between 0.309 and 0.351. However, the optimum solution for the small office is characterized by a medium WU of 3.8 W/m<sup>2</sup>·K compared with high WUs of 5.85 W/m<sup>2</sup>·K for the medium and large offices. The above changes in design preferences are summarized in Table 7. Changing plan sizes from small to large scales is equivalent to decreasing the shape coefficient from 0.17 to 0.08, which can explain the similarity with the scenario of changing plan shapes. In addition, changing the plan size also varies the area ratio of internal and perimeter zones, which is another rationale behind the observed impact. Fig. 16 shows a breakdown of HVAC energy demands for different thermal zones. It can be clearly seen that passive design strategies mainly affect the air-conditioning load of perimeter zones as indicated by the high energy-saving potential from 39.70% to 54.64% dependent on window orientations. South-facing perimeter zones have the highest energy-saving potential which is determined by the sun exposure condition of the external façade. In contrast, the energy demand of internal zones can only be slightly reduced by passive design strategies with a maximum energy-saving potential of 17.73%. As a result, the total energy-saving potential decreases with the increased area of the internal zone and the corresponding larger contribution to the air-conditioning load up to 67.27%.

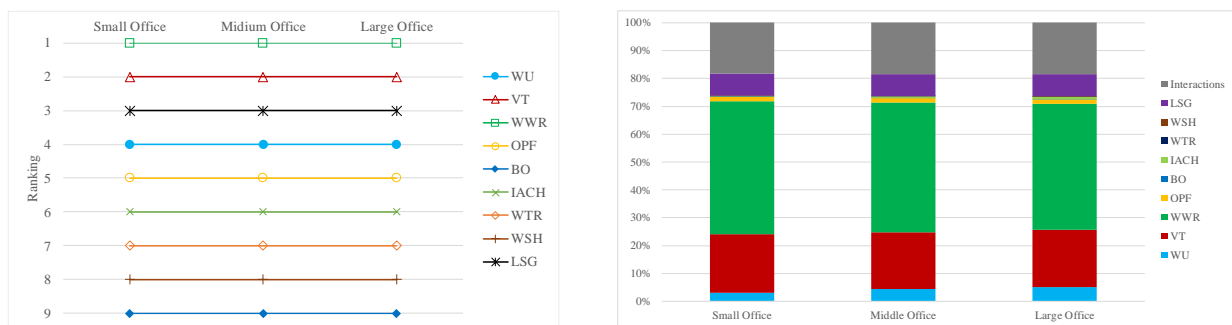


Fig. 14. Impact of plan size on factor prioritizing



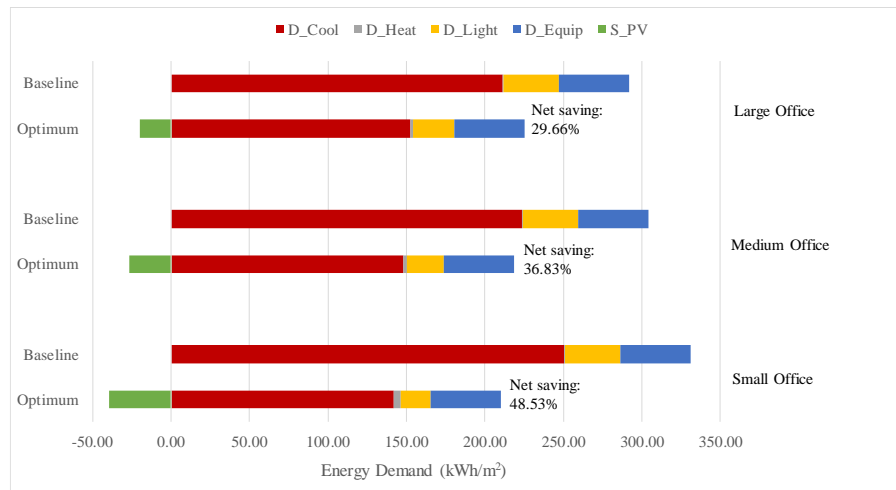
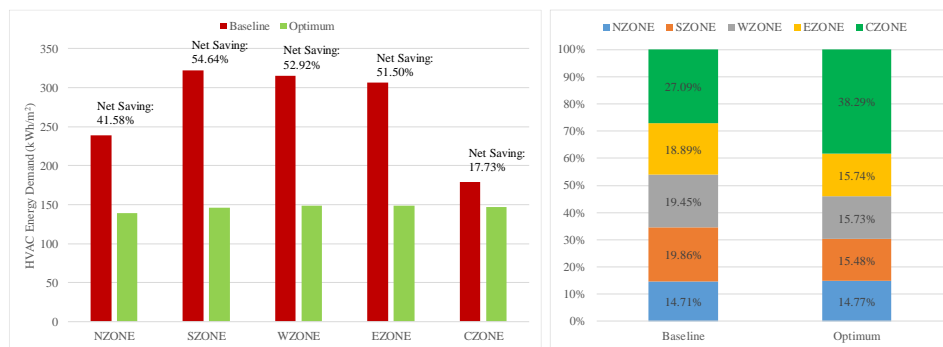
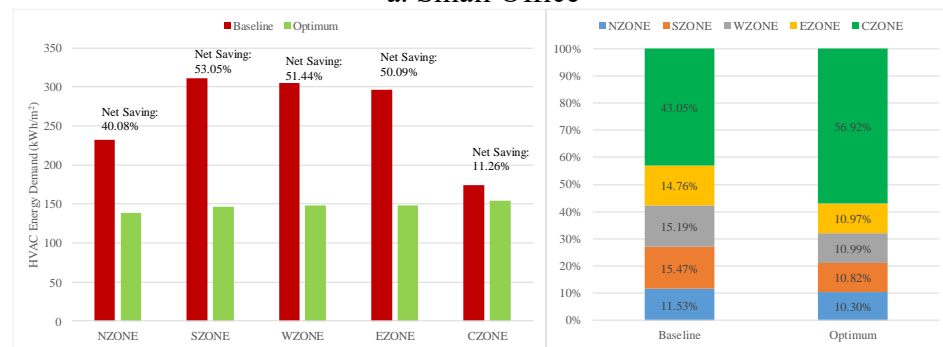


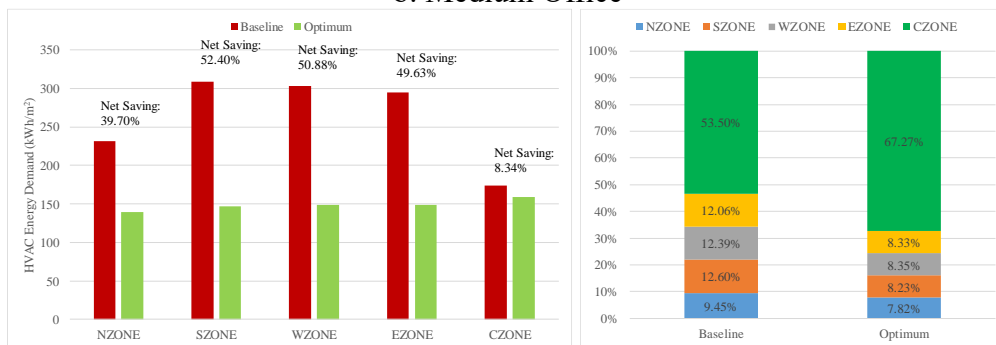
Fig. 15. Comparison of baseline and design energy performances of different plan sizes



a. Small Office



b. Medium Office



c. Large Office

Fig. 16. Breakdown of energy demand for thermal zones

Table 7. Optimum design solutions for different plan shapes

	SC -	D_Light (kWh/m <sup>2</sup> )	D_HVAC (kWh/m <sup>2</sup> )	S_PV (kWh/m <sup>2</sup> )	WU (W/m <sup>2</sup> ·K)	VT -	WWR -	LSG -
Small office	0.17	19.005	146.217	39.562	3.800	0.351	0.10	2.4
Medium office	0.11	23.335	150.388	26.424	5.850	0.323	0.10	2.4
Large office	0.08	25.926	154.465	19.837	5.850	0.309	0.10	2.4

Note: Lighting energy demand - D\_Light; HVAC energy demand - D\_HVAC; PV energy supply - S\_PV

### 3.5. Impact of urban contexts

Unlike the impact of archetypes, urban contexts have a conspicuous influence over the factor prioritizing result as shown in Fig. 17. The ranking of window and shading related design parameters has been greatly changed, while the exact contribution of each design input varies by up to 20%. Because of the increased peripheral shading in urban contexts with higher densities (i.e. higher building height to street width ratios: H/W), the influence of the window size (WWR) and visible light transmittance (VT) are substantially decreased by 18.40% and 8.06%, while the influence of the window thermal properties (WU) is tremendously increased by 19.09%. With less exposure to solar radiation, the thermal insulation performance becomes more important to energy efficient designs. The wall thermal resistance (WTR) can also make a unique contribution up to 11.83% in high-density contexts. Meanwhile, the influence of the infiltration/ventilation (IACH) is also increased by 3.31%, making it a significant design factor in medium and high density urban contexts. The window shading (OPF) also becomes a significant design factor in low and medium density contexts due to an increased interactive effect with other design variables.

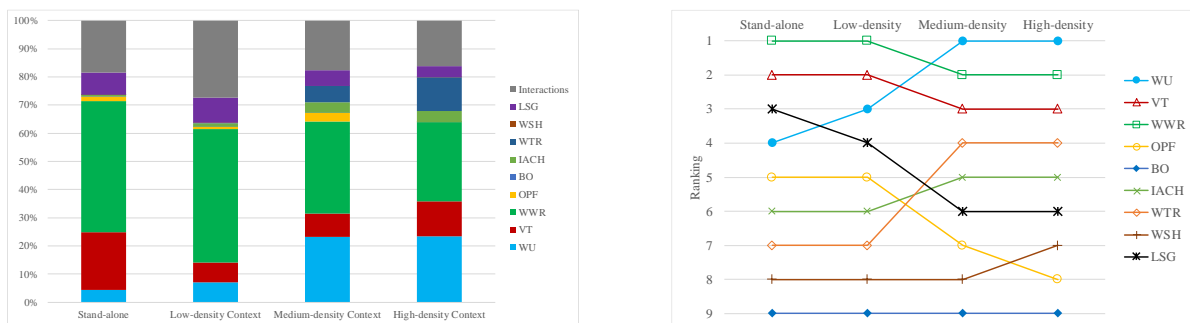


Fig. 17. Impact of urban contexts on factor prioritizing

Furthermore, optimization results and energy performances of both baseline and optimum scenarios are also affected by urban contexts. As shown in Fig. 18, the net energy-saving potential compared with the baseline decreases from 36.83% of the stand-alone scenario to 8.62% of the high-density context scenario. Meanwhile, H/W increases from 0.0 of the stand-alone case to 12 of the high-density case. Lighting and equipment energy demands maintain constant for all baseline designs, while the lighting demand of optimum designs varies between 23.335 and 35.244 kWh/m<sup>2</sup> by up to 51.03% in different urban contexts. HVAC energy demands of baseline designs vary in a broad range between 224.067 and 165.407 kWh/m<sup>2</sup>, whereas those of optimum designs fluctuate within 1.12% between 149.934 and 152.068 kWh/m<sup>2</sup>. On the supply side, the PV power generation of optimum designs varies from 5.331 to 26.424 kWh/m<sup>2</sup> by up to 79.82%.

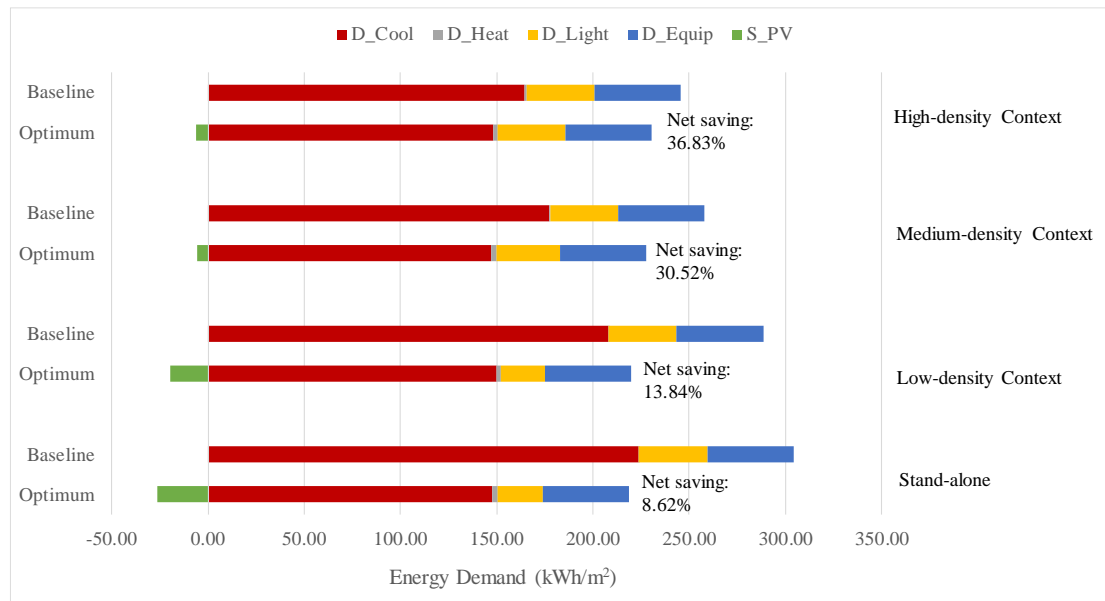


Fig. 18. Comparison of baseline and design energy performances of different urban contexts

In terms of the design space for optimum solutions, all building designs in different contexts are characterized by a high LSG of 2.4 but have diverse preferences for other significant design parameters. In the low-density context, the optimum design is characterized by a slightly larger WWR of 0.12, an increased VT of 0.661, an OPF of 0.139 and a decreased WU of 3.4 W/m<sup>2</sup>·K. In the medium-density context, the optimum design is characterized by a lower VT of 0.24, a much larger WWR of 0.62, a high WTR of 6.25 m<sup>2</sup>·K/W and IACH of 1.5 h<sup>-1</sup>. The optimum design for the high-

density urban context is similar to that for the medium-density context, except that WWR and WTR are extensively reduced. The above changes in design preferences are summarized in Table 8. Changing the urban context not only affects design preferences but also changes the dimension of the optimization problem as per the factor-fixing result. Passive architectural design strategies are generally less effective in a heavily shaded building project site, highlighting the importance of the site selection and building setback in the urban environment [15]. The high uncertainty of both sensitivity indices and optimum solutions with the varied urban context revealed its critical role in energy-efficient building designs. In future study, more complex urban morphologies will be introduced with the combination of the GIS software and surrogate building model, so that more realistic shading and thermal load modelling can be achieved within a reasonable computation time.

Table 8. Optimum design solutions for different urban contexts

	Stand-alone	Low-density	Medium-density	High-density
H/W (-)	0	1	3.75	12
D_Light (kWh/m <sup>2</sup> )	23.335	23.005	32.923	35.244
D_HVAC (kWh/m <sup>2</sup> )	224.067	208.356	177.976	165.407
S_PV (kWh/m <sup>2</sup> )	26.424	19.495	5.331	6.189
WU (W/m <sup>2</sup> ·K)	5.85	3.4	5.85	5.85
VT (-)	0.323	0.661	0.240	0.240
WWR (-)	0.10	0.12	0.62	0.10
LSG (-)	2.4	2.4	2.4	2.4
OPF (-)	0#	0.139	0	0#
WTR (m <sup>2</sup> ·K/W)	0.136#	0.136#	6.25	0.176
IACH (h <sup>-1</sup> )	0.5#	0.5#	1.5	1.5

Note<sup>1</sup>: # indicates non-significant parameters fixed to baseline values in optimization

Note<sup>2</sup>: Lighting energy demand - D\_Light; HVAC energy demand - D\_HVAC; PV energy supply - S\_PV

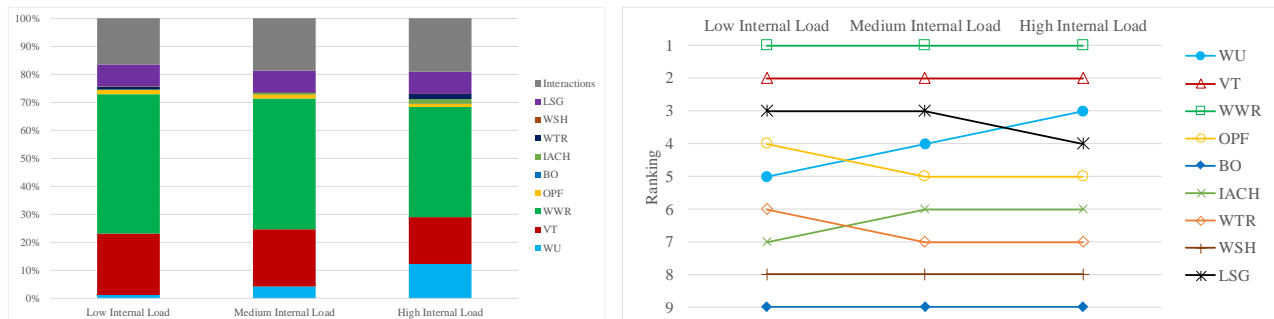


Fig. 19. Impact of internal loads on factor prioritizing

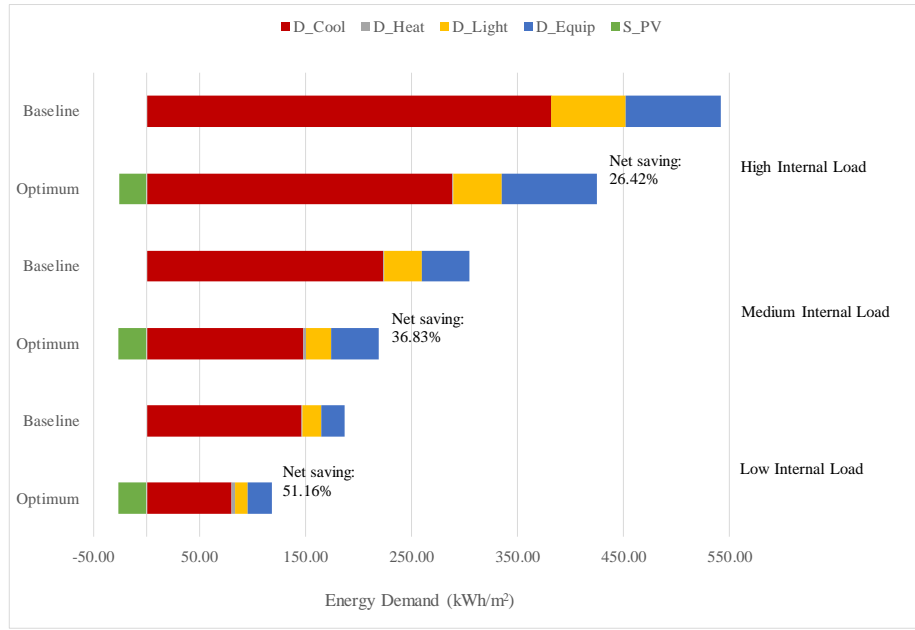


Fig. 20. Comparison of baseline and design energy performances of different internal loads

### 3.6. Impact of internal load

Internal load (heat gain) levels can also change factor prioritizing results as shown in Fig. 19. The ranking of the window U-value (WU) has been greatly changed with its exact contribution increased by 11.12% from the low internal load to high internal load level. WU is even removed from the optimization problem space in the low internal load scenario. The contribution of VT and WWR is correspondingly reduced by 5.31% and 10.37% with increased load levels. Optimization results and energy performances of both baseline and optimum scenarios are also greatly influenced by changing internal loads. As shown in Fig. 20, the net energy-saving potential (from 26.42% to 51.16%) is approximately inversely proportioned to peak load levels. Apart from the HVAC demand of optimum designs, other energy demands are also approximately scaled up with internal load levels. On the supply side, the PV power generation fluctuates slightly between 25.907 and 26.516 kWh/m<sup>2</sup> which is mainly influenced by different design preferences of VT. In terms of the design space for optimum solutions, all building designs prefer a small WWR around 10% and a high LSG of 2.4. However, VT for optimum solutions is increased from 0.263 to 0.622 with growing internal load levels. WU is not identified as a critical design factor in the low internal load case, while it decreases from 5.850 W/m<sup>2</sup>·K of the medium internal load case to 3.413 W/m<sup>2</sup>·K of the high internal load case. The above changes in design preferences are summarized in Table 9. The role of window U-value

(WU) becomes critical when the conductive and convective heat transfer through windows is increased with growing internal heat gains. The plug-load (equipment consumption) alone was not considered to impact the design preference in a previous parametric study [20], which contradicts with findings in this research. The discrepancy might be attributed to the fact that the lighting and occupant heat gain was not considered in their study so that the possible variation range of internal loads was rather narrow.

Table 9. Optimum design solutions for different internal loads

	Peak load W/m <sup>2</sup>	D_Light (kWh/m <sup>2</sup> )	D_HVAC (kWh/m <sup>2</sup> )	S_PV (kWh/m <sup>2</sup> )	WU (W/m <sup>2</sup> ·K)	VT -	WWR -	LSG -
Low internal load	18.5	11.869	83.449	26.516	2.630#	0.263	0.10	2.4
Medium internal load	37	23.335	150.388	26.424	5.850	0.323	0.10	2.4
High internal load	74	45.190	289.692	25.907	3.413	0.662	0.10	2.4

Note<sup>1</sup>: # indicates non-significant parameters fixed to baseline values in optimization  
Note<sup>2</sup>: Lighting energy demand - D\_Light; HVAC energy demand - D\_HVAC; PV energy supply - S\_PV

## 4. Conclusions

This paper thoroughly investigated uncertainties of sensitivity analyses and design optimizations of a low-energy commercial building under diverse archetypes and confounding factors. Selected key passive architectural design parameters are subject to Monte Carlo sampling based on a developed simulation platform combining EnergyPlus, JEPlus, R and GenOpt. The impact of building shapes, sizes, urban contexts and internal loads (heat gain) on both baseline and optimum building designs is evaluated while the energy-saving potential of the integrated photovoltaic envelope is explored. Findings from this research can serve as guidelines for the green building design and benchmarking in a sustainable neighborhood planning background. Major achievements are summarized as follows:

- 1) A reference high-rise commercial building model is developed by coupling photovoltaic panels with both transparent and opaque building envelopes while modelling experiments were designed by varying independent and dependent passive design parameters randomly in their whole possible distribution ranges. The reference building model was adapted from ASHRAE 90.1 prototypes to represent the local building design practice in Hong Kong. The model was successfully benchmarked with official energy end-use statistics so that it can represent the

energy performance of an average office building with an acceptable deviation of 3.52%.

- 2) Based on qualitative and quantitative sensitivity analyses conducted on the reference case, all design parameters except the wall thermal resistance (WTR) are proved to have a close to monotonic relationship with the net energy demand. Window thermal and geometric properties including the window U-value (WU), visible transmittance (VT), light to solar gain ratio (LSG) and window to wall ratio (WWR) are identified as significant design factors based on bootstrapped FAST total-order indices. WWR alone contributes to nearly half of the variation in the model output, because it can simultaneously influence the HVAC, lighting and PV energy. The hybrid generalized pattern search particle swarm optimization (HGPPSO) is then performed on the reduced problem space and achieves a net energy demand reduction of 36.83% compared to the baseline design. The optimum design shows a preference for a small window size and light transmittance while a high light to solar gain ratio and window U-value.
- 3) The building plan shape is proved to have a minor influence over the factor prioritizing result for the integrated PV envelope design. The ranking with Morris maintains constant, while FAST first-order indices fluctuate slightly within 1%. However, the energy-saving potential can vary from 36.83% of the reference square design to 48.77% of the H-shape design. Design scenarios with higher shape coefficients have a higher energy-saving potential in HVAC and lighting and can produce more PV power irrespective of the increased self-shading effect. An ideal linear regression equation with a  $R^2$  of 0.959 is obtained for the correlation between HVAC demands and shape coefficients. It is indicated that the negative effect of larger external facade areas overwhelmed the positive effect of self-shading. Optimum designs under varied shape coefficients also showed different preferences of window thermal and optical properties.
- 4) The variation of floor plan sizes can also be translated to the variation of shape coefficients so that its impact on factor prioritizing is quite similar. In addition, the variation of floor sizes also changes the area ratio between perimeter zones and internal zones. Because the energy-saving potential of internal zones is much lower than that of perimeter zones, the reduced energy-saving potential in larger floor sizes can also be attributed to the increased proportion of internal zones.
- 5) The urban context can greatly impact factor prioritizing results. The contribution of WWR and VT to the net energy demand is substantially reduced by 18.40% and 8.06%, while the

contribution of WU is increased by 19.09% with heavier peripheral shading in high-density contexts. Judging by bootstrapped FAST total-order indices, OPF also becomes a significant design factor for low and medium density urban contexts when local shading becomes important to solar gain control. The infiltration/ventilation (IACH) and wall thermal insulation (WTR) also become important design factors with an individual contribution up to 11.83% in medium and high density urban contexts. The energy-saving potential of the whole building is greatly reduced in a high-density scenario, indicating the necessity of a cautious site selection and setback design in the early planning stage for maximizing the benefit of passive design strategies. Moreover, optimum solutions under diverse urban contexts also showed different preferences of the window size.

- 6) At last, the internal load is validated to have a solid influence over factor prioritizing, where the contribution of WU is increased by up to 11.12% with growing peak internal heat gain. The U-value of windows becomes significant with more conductive and convective heat transfer through the envelope in higher internal load conditions. The energy demand and energy-saving potential are both approximately linearly correlated with the peak internal load. The observed impact of internal loads contradicts with conclusion in existing literature, indicating the necessity of including occupant and lighting heat gain in the sensitivity analysis.

This work proposed a holistic and efficient early-stage building energy optimization approach by closely incorporating PV envelopes with conventional passive architectural designs under variable urban contexts and design scenarios. Such an approach can be used to reduce the design optimization cost and facilitate swift decision-making for deploying construction resources in a green building project. Major findings from this research can assist in renovating the energy end-use benchmark for commercial buildings in Hong Kong and provide comprehensive design guidelines for integrated PV facade applications.

## **Acknowledgment**

The work described in this paper was supported by the Innovation and Technology Fund with project No. ITS/171/16FX and the Postdoctoral Fellow Scheme of the Faculty of Construction and Environment, The Hong Kong Polytechnic University (Grant No.: K-ZM2G). Appreciation was also



given to the National Key R&D Program of China, Research and Demonstration of Key Technology of Net-Zero Energy Building (Project No.: 2016YFE0102300).

## Nomenclatures

### *Abbreviation*

<i>BEAM</i>	building environment assessment method
<i>BO</i>	building orientation
<i>FAST</i>	Fourier amplitude sensitivity test
<i>GPVA</i>	active glazing PV area
<i>GPS</i>	generalized pattern search
<i>HGPSPO</i>	hybrid generalized pattern search particle swarm optimization
<i>HVAC</i>	heating ventilation and air conditioning
<i>IACH</i>	infiltration air change per hour
<i>IWEC</i>	international weather for energy calculations
<i>LEED</i>	leadership in energy and environmental design
<i>LSG</i>	light to solar gain ratio
<i>OTTV</i>	overall thermal transfer value
<i>OPF</i>	overhang projection fraction
<i>PSO</i>	particle swarm optimization
<i>PV</i>	photovoltaic
<i>SA</i>	sensitivity analysis
<i>SC</i>	shading coefficient
<i>SHGC</i>	solar heat gain coefficient
<i>VIF</i>	variance inflation factor
<i>VT</i>	visible transmittance
<i>WGR</i>	window to ground ratio
<i>WPVA</i>	active wall PV area
<i>WSH</i>	wall specific heat
<i>WTR</i>	wall thermal resistance
<i>WU</i>	window U-value
<i>WWR</i>	window to wall ratio

## References

- [1] EMSD. Hong Kong Energy End-use Data 2018. Electrical & Mechanical Services Department. <http://www.emsd.gov.hk>; 2018.
- [2] Chung W. Review of building energy-use performance benchmarking methodologies. *Applied Energy*. 2011;88:1470-9.
- [3] Yik FWH, Wan KSY. An evaluation of the appropriateness of using overall thermal transfer value (OTTV) to regulate envelope energy performance of air-conditioned buildings. *Energy*. 2005;30:41-71.
- [4] Lee WL, Yik FWH, Burnett J. Assessing energy performance in the latest versions of Hong Kong Building Environmental Assessment Method (HK-BEAM). *Energy and Buildings*. 2007;39:343-54.
- [5] Delgarm N, Sajadi B, Kowsary F, Delgarm S. Multi-objective optimization of the building energy performance: A simulation-based approach by means of particle swarm optimization (PSO).

Applied Energy. 2016;170:293-303.

[6] Mangkuto RA, Rohmah M, Asri AD. Design optimisation for window size, orientation, and wall reflectance with regard to various daylight metrics and lighting energy demand: A case study of buildings in the tropics. *Applied Energy*. 2016;164:211-9.

[7] Harmathy N, Magyar Z, Folić R. Multi-criterion optimization of building envelope in the function of indoor illumination quality towards overall energy performance improvement. *Energy*. 2016;114:302-17.

[8] Zhang A, Bokel R, van den Dobbelsteen A, Sun Y, Huang Q, Zhang Q. Optimization of thermal and daylight performance of school buildings based on a multi-objective genetic algorithm in the cold climate of China. *Energy and Buildings*. 2017;139:371-84.

[9] Zhang L, Zhang L, Wang Y. Shape optimization of free-form buildings based on solar radiation gain and space efficiency using a multi-objective genetic algorithm in the severe cold zones of China. *Solar Energy*. 2016;132:38-50.

[10] Negendahl K, Nielsen TR. Building energy optimization in the early design stages: A simplified method. *Energy and Buildings*. 2015;105:88-99.

[11] Chan ALS. Effect of adjacent shading on the thermal performance of residential buildings in a subtropical region. *Applied Energy*. 2012;92:516-22.

[12] Premrov M, Žegarac Leskovar V, Mihalič K. Influence of the building shape on the energy performance of timber-glass buildings in different climatic conditions. *Energy*. 2016;108:201-11.

[13] Konis K, Gamas A, Kensek K. Passive performance and building form: An optimization framework for early-stage design support. *Solar Energy*. 2016;125:161-79.

[14] Méndez Echenagucia T, Capozzoli A, Cascone Y, Sassone M. The early design stage of a building envelope: Multi-objective search through heating, cooling and lighting energy performance analysis. *Applied Energy*. 2015;154:577-91.

[15] Martins TAdL, Adolphe L, Bastos LEG, Martins MAdL. Sensitivity analysis of urban morphology factors regarding solar energy potential of buildings in a Brazilian tropical context. *Solar Energy*. 2016;137:11-24.

[16] Han Y, Taylor JE, Pisello AL. Exploring mutual shading and mutual reflection inter-building effects on building energy performance. *Applied Energy*. 2017;185, Part 2:1556-64.

[17] Lima I, Scalco V, Lamberts R. Estimating the impact of urban densification on high-rise office building cooling loads in a hot and humid climate. *Energy and Buildings*. 2019;182:30-44.

[18] Allegrini J, Dorer V, Carmeliet J. Impact of radiation exchange between buildings in urban street canyons on space cooling demands of buildings. *Energy and Buildings*. 2016;127:1074-84.

[19] Erell E, Pearlmutter D, Boneh D, Kutiel PB. Effect of high-albedo materials on pedestrian heat stress in urban street canyons. *Urban Climate*. 2014;10:367-86.

[20] Samuelson H, Claussnitzer S, Goyal A, Chen Y, Romo-Castillo A. Parametric energy simulation in early design: High-rise residential buildings in urban contexts. *Building and Environment*. 2016;101:19-31.

[21] Jenkins DP. The importance of office internal heat gains in reducing cooling loads in a changing climate. *International Journal of Low-Carbon Technologies*. 2009;4:134-40.

[22] Lam JC. Shading effects due to nearby buildings and energy implications. *Energy Conversion and Management*. 2000;41:647-59.

[23] Lam JC, Chan RYC, Tsang CL, Li DHW. Electricity use characteristics of purpose-built office buildings in subtropical climates. *Energy Conversion and Management*. 2004;45:829-44.

- [24] Chan ALS, Chow TT, Fong KF, Lin Z. Investigation on energy performance of double skin façade in Hong Kong. *Energy and Buildings*. 2009;41:1135-42.
- [25] Chen X, Yang H, Sun K. Developing a meta-model for sensitivity analyses and prediction of building performance for passively designed high-rise residential buildings. *Applied Energy*. 2017;194:422-39.
- [26] Gueymard CA, duPont WC. Spectral effects on the transmittance, solar heat gain, and performance rating of glazing systems. *Solar Energy*. 2009;83:940-53.
- [27] Zhai Z, Johnson M-H, Krarti M. Assessment of natural and hybrid ventilation models in whole-building energy simulations. *Energy and Buildings*. 2011;43:2251-61.
- [28] Schulze T, Eicker U. Controlled natural ventilation for energy efficient buildings. *Energy and Buildings*. 2013;56:221-32.
- [29] Chen X, Yang H. Combined thermal and daylight analysis of a typical public rental housing development to fulfil green building guidance in Hong Kong. *Energy and Buildings*. 2015;108:420-32.
- [30] ASHARE 90.1: Energy Standard for Buildings Except Low-Rise Residential Buildings. ASHRAE; 2013.
- [31] Nabil A, Mardaljevic J. Useful daylight illuminances: A replacement for daylight factors. *Energy and Buildings*. 2006;38:905-13.
- [32] Wang M, Peng J, Li N, Yang H, Wang C, Li X, et al. Comparison of energy performance between PV double skin facades and PV insulating glass units. *Applied Energy*. 2017;194:148-60.
- [33] Peng J, Lu L, Yang H, Han J. Investigation on the annual thermal performance of a photovoltaic wall mounted on a multi-layer façade. *Applied Energy*. 2013;112:646-56.
- [34] Petter Jelle B, Breivik C, Drolsum Røkenes H. Building integrated photovoltaic products: A state-of-the-art review and future research opportunities. *Solar Energy Materials and Solar Cells*. 2012;100:69-96.
- [35] Balter J, Ganem C, Discoli C. On high-rise residential buildings in an oasis-city: Thermal and energy assessment of different envelope materiality above and below tree canopy. *Energy and Buildings*. 2016;113:61-73.
- [36] Chen Y, Hong T. Impacts of building geometry modeling methods on the simulation results of urban building energy models. *Applied Energy*. 2018;215:717-35.
- [37] Chen Y, Hong T, Piette MA. Automatic generation and simulation of urban building energy models based on city datasets for city-scale building retrofit analysis. *Applied Energy*. 2017;205:323-35.
- [38] Chen X, Yang H. A multi-stage optimization of passively designed high-rise residential buildings in multiple building operation scenarios. *Applied Energy*. 2017;206:541-57.
- [39] Huang J, Chen X, Yang H, Zhang W. Numerical investigation of a novel vacuum photovoltaic curtain wall and integrated optimization of photovoltaic envelope systems. *Applied Energy*. 2018;229:1048-60.
- [40] Menberg K, Heo Y, Choudhary R. Sensitivity analysis methods for building energy models: Comparing computational costs and extractable information. *Energy and Buildings*. 2016;133:433-45.
- [41] Cukier RI, Levine HB, Shuler KE. Nonlinear sensitivity analysis of multiparameter model systems. *Journal of Computational Physics*. 1978;26:1-42.
- [42] Saltelli A, Tarantola S, Chan KPS. A Quantitative Model-Independent Method for Global

Sensitivity Analysis of Model Output. *Technometrics*. 1999;41:39-56.

[43] Deb K. Multi-objective optimization using evolutionary algorithms. 1st ed. Chichester, New York, N.Y: John Wiley & Sons; 2001.

[44] Bououden S, Chadli M, Karimi HR. An ant colony optimization-based fuzzy predictive control approach for nonlinear processes. *Information Sciences*. 2015;299:143-58.

[45] Si Y, Karimi HR, Gao H. Modelling and optimization of a passive structural control design for a spar-type floating wind turbine. *Engineering Structures*. 2014;69:168-82.

[46] Wetter M. Generic Optimization Program User Manual Version 3.1.1. Lawrence Berkeley National Laboratory. 2016.

[47] Kaur A, Kaur M. A Review of Parameters for Improving the Performance of Particle Swarm Optimization 2015.

[48] Chung W, Hui YV. A study of energy efficiency of private office buildings in Hong Kong. *Energy and Buildings*. 2009;41:696-701.

[49] Garcia Sanchez D, Lacarri re B, Musy M, Bourges B. Application of sensitivity analysis in building energy simulations: Combining first- and second-order elementary effects methods. *Energy and Buildings*. 2014;68:741-50.

[50] A. Saltelli MR, Terry Andres, Francesca Campolongo, Jessica Cariboni, Debora Gatelli, Michaela Saisana, Stefano Tarantola. *Global Sensitivity Analysis: The Primer*: John Wiley & Sons Ltd; 2008.

[51] Yang L, Lam JC, Tsang CL. Energy performance of building envelopes in different climate zones in China. *Applied Energy*. 2008;85:800-17.